A NOVEL NONLINEAR FEEDBACK CONTROL AND ITS APPLICATION TO COURSE-KEEPING AUTOPILOT

Xian-Ku Zhang
Navigation College, Dalian Maritime University, Dalian, Liaoning province, Republic of China

Guo-Qing Zhang
Navigation College, Dalian Maritime University, Dalian, Liaoning province, Republic of China., zgq_dlmu@163.com

Xiu-Jia Chen
Navigation College, Dalian Maritime University, Dalian, Liaoning province, Republic of China

A NOVEL NONLINEAR FEEDBACK CONTROL AND ITS APPLICATION TO COURSE-KEEPING AUTOPILOT

Acknowledgements

A NOVEL NONLINEAR FEEDBACK CONTROL AND ITS APPLICATION TO COURSE-KEEPING AUTOPILOT

Xian-Ku Zhang, Guo-Qing Zhang*, and Xiu-Jia Chen

ABSTRACT

Over the past years, more and more concentration has been attended on developing novel control algorithms to stabilize or regulate the practical plant. In this note, a novel technique is presented to improve the control performance by modulating the output error using a sine function. This nonlinear feedback signal is sent to the original control law instead of the output error itself, which is the derivation between the system output and the reference signal. That is the so-called nonlinear feedback control technique. By virtue of the describing function and the robust control theory, the theoretical analysis shows that the minor control efforts are required to obtain the same control performance due to the merit of the nonlinear feedback scheme. Simulation experiment based on "YULONG" vessel is presented to illustrate the effectiveness of the proposed algorithm.

I. INTRODUCTION

The application of surface vessels is increasing globally due to its superiorities on capacity and economy (Fossen, 2011; Ueno et al., 2014). Based on a marine literature review (Sorensen, 2011), the course keeping control for ships has been a benchmark problem in the field of marine cybernetics. And it plays an important role in marine transportation and oceanic exploration.

The history of automated course keeping control started with Elmer Sperry, who constructed the first automatic ship steering mechanism in 1911 (Bennet, 1979; Sorensen, 2011). This technique is referred to as the "Metal Mike", and could capture the behavior of a skilled pilot or helmsman. Later in 1922, Nicholas Minorsky proposed a three-term control law to implement the control task, i.e. the Proportional-Integral-Derivative (PID) control (Benneff, 1984). In recent years, more practical conditions are considered in the research work on the course keeping control, e.g. the varying sea states and the unknown system nonlinearity. In reference (Du et al., 2007), an adaptive course keeping controller was proposed for the time varying parametric uncertain nonlinear ships with completely unknown bounded parameters. The method did not require a priori knowledge of the sign of the unknown time varying control gain. Unlike the online optimal based scheme (Ho et al., 2010), the heading autopilot in (Velasco et al., 2013) was developed based on an autonomous In-Scale Fast Ferry. The physical control system was implanted by using Wi-Fi communications, and the research work was very valuable for the course keeping control design. In addition, robust scheme is also a powerful tool to implement the control task. The reference (Satpati et al., 2008) presented a design of the robust course controller for a cargo ship by employing the Particle Swarm Optimization (PSO) enabled automated Quantitative Feedback Theory (QFT), which had considered the impact of the uncertain environment. The plant dynamics was described as a second order Nomoto model with structure parametric variation, and the simulation result illustrated the validity of the algorithm. By virtue of the robust least squares support vector machine, an robust course keeping control algorithm was developed in (Ihle et al., 2006), which made full use of the nonlinear mapping ability, self-learning adaptability and parallel information processing of the least squares support vector machine. In this scheme, the H_2/H_∞ robust method was incorporated to obtain the good stabilizing performance to the sea condition variation.

Note that the aforementioned works is all based on the linear feedback control. That is, the input signal to the control law is proportional to the output error, even including the existed nonlinear control schemes aiming to the nonlinear plant with more general form (Marino and Tomei, 2013; Ginoya et al., 2015). For a smaller output error, the action derived by the control law may be not enough, while it is too strong for the case of the larger output error. However, that may be not completely mapping to the practical condition. In the marine control engineering, a small rudder amplitude and
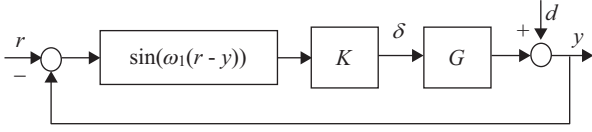
Fig. 1. Configuration of a nonlinear feedback system.

slow rudder ratio mean energy saving and abrasion reduction of the steering engine. Furthermore, the steering operation at cost of the large rudder angle can lead to the increased rolling amplitude, which is a threat to the navigation safety (Zhang and Wang, 2010; Zhang, 2012). Thus, even to the more general plant, the initial control input and the steering frequency are required to be as small as possible.

Motivated by the above observations, a novel nonlinear feedback control is proposed by employing the sine function of error between the reference signal and the actual output as the input of the control law. Different from the routine linear feedback control, it is an essential nonlinear feedback control technique. With the proposed scheme, the same performance can be obtained with the minor control action on the basis of the unchanged controller. The effectiveness of the developed algorithm has been validated through the theoretical analysis and the simulation experiments.

II. NONLINEAR FEEDBACK CONTROL SYSTEM DRIVEN BY SINE FUNCTION

A nonlinear feedback system driven by sine function is shown in Fig. 1, contrary to the standard feedback configuration. $\sin(\omega_1(r-y))$ is introduced in the scheme instead of $r-y$, where ω_1 is the dimensionless system frequency. Note that the block diagram of $\sin(\omega_1(r-y))$ shown in Fig. 1 does not conform to its standard graphical representation. How to find a stable K with fine control performance in $\delta = K(r-y)$ is the main work in the existed research work, no matter the controller K is linear or nonlinear. Even though, the objective of this note is to access the better control performance of the nonlinear feedback control with the mathematical form of $\delta = K\sin(\omega_1(r-y))$ under the same controller K.

Consider the course keeping control task for marine ships, the plant G is taken as the nominal Nomoto model when the control law K is designed using the first-order closed loop gain shaping algorithm (Zhang, 2012; Zhang et al., 2014) without considering the nonlinear feedback. Robust controller of a standard feedback system is solved by configuring reasonably three predetermined conditions: the bandwidth frequency of the closed system being $1/T_1$ ($1/T_1$ should be crossover frequency in the strict sense, and is approximately regarded as the bandwidth frequency for the sake of easy analysis), the largest singular value being unity, and the high frequency asymptote slope being -20 dB/dec. In consequence, the frequency spectrum of the closed-loop system is equal to the frequency spectrum of a first-order inertial system with the largest

singular value 1 approximately, i.e.

$$\frac{1}{T_1 s + 1} = \frac{GK}{1+GK} \qquad (1)$$

and the actual course keeping control law is derived as Eq. (2).

$$K = \frac{1}{GT_1 s} \qquad (2)$$

The ship model being a standard Nomoto model is expressed in Eq. (3), where ψ is the heading angle and δ is the rudder angle, K_0, T_0 are the maneuverability indices of marine ships.

$$G(s) = \frac{\psi}{\delta} = \frac{K_0}{s(T_0 s + 1)} \qquad (3)$$

In order to ensure the closed loop gain shaping algorithm shown in Eq. (1) with the capability of eliminating the steady state error, a minor constant ε (0.01) is incorporated into the denominator of Nomoto model (3). ε reproduces the effect of eliminating uncertain constant disturbance upon the ship motion. The actual model for the control design is presented as Eq. (4).

$$G(s) = \frac{K_0}{T_0 s^2 + s + \varepsilon} \qquad (4)$$

Thus, substituting Eq. (4) into Eq. (2), the linear PID controller (5) can be obtained.

$$K(s) = \frac{1}{K_0 T_1} + \frac{\varepsilon}{K_0 T_1 s} + \frac{T_0}{K_0 T_1} s \qquad (5)$$

In actual application, one could note that the settling time is relatively long for marine ships with large time constants, e.g. oil tankers, etc. The dynamical performance of the course keeping control system can be improved greatly when the proportional part of the PID law (5) has an added positive variable ρ. The practical control law could be described as Eq. (6). Around this design, the corresponding theoretical analysis and test experiments are given in reference (Zhang and Guan, 2010).

$$K(s) = \left(\frac{1}{K_0 T_1} + \rho\right) + \frac{\varepsilon}{K_0 T_1 s} + \frac{T_0}{K_0 T_1} s \qquad (6)$$

In Fig. 1, the effects of nonlinear feedback to the dynamic and static performance are analyzed by using $\sin(\omega_1(r-y)) \approx \omega_1(r-y)$ when the error is small. The corresponding demonstration is presented in (Zhang, 2011). In some situations, the

approximation $\sin(\omega_1(r-y)) \approx \omega_1(r-y)$ may not be tenable when the error is large. The effects of nonlinear feedback driven by sine function to the closed system can be analyzed by Taylor series expansion, i.e. Eq. (7).

$$\sin\left(\omega_1\left(r-y\right)\right) \approx \omega_1\left(r-y\right) - \frac{\left(\omega_1\left(r-y\right)\right)^3}{3!} + \frac{\left(\omega_1\left(r-y\right)\right)^5}{5!} - \cdots \tag{7}$$

Define the output error $e = r - y$, Eq. (7) is simplified up to third-order. Then, Eq. (8) can be obtained.

$$f(e) = \omega_1 e - \frac{\omega_1^3}{6} e^3 \tag{8}$$

According to the reference (Hu, 2007), if the output error e of Eq. (8) is $A\sin\omega_0 t$, then the output of the nonlinear system in Eq. (8) can be described by its first-order harmonic element, and the equivalent frequency characteristics is the describing function of the nonlinear system.

Define the output of Eq. (8) as $f(t)$ under the sine input $A\sin\omega_0 t$, then it can be expressed using its first-order harmonic element (Zhang, 2011):

$$f(t) = A_0 + A_1 \cos\omega_0 t + B_1 \sin\omega_0 t \tag{9}$$

where A_0 is the DC component, A_1, B_1 are the first-order harmonic components, and

$$\begin{cases} A_0 = \dfrac{1}{2\pi} \displaystyle\int_0^{2\pi} f(t)\mathrm{d}\omega_0 t, \\[2mm] A_1 = \dfrac{1}{\pi} \displaystyle\int_0^{2\pi} f(t)\cos\omega_0 t\,\mathrm{d}\omega_0 t, \\[2mm] B_1 = \dfrac{1}{\pi} \displaystyle\int_0^{2\pi} f(t)\sin\omega_0 t\,\mathrm{d}\omega_0 t \end{cases} \tag{10}$$

Under the action of sine input signal e in Eq. (7), the complex ratio of its first-order harmonic element in the steady state output to its input signal is referred to the describing function which is expressed as $N(A)$.

$$N(A) = \frac{B_1 + jA_1}{A} \tag{11}$$

Eq. (8) is an odd function, thus $A_0 = 0$. As to $e = A\sin\omega_0 t$,

$$f(t) = \omega_1 A\sin\omega_0 t - \frac{\omega_1^3 A^3}{6}\sin^3\omega_0 t \tag{12}$$

Eq. (12) is also an odd function of t, so $A_1 = 0$. Because of the semi-cyclic symmetry property of $f(t)$, then

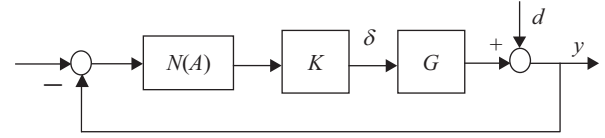**Fig. 2. Equivalent configuration of a nonlinear feedback system.**

$$\begin{aligned} B_1 &= \frac{4}{\pi} \int_0^{\pi/2} f(t)\sin\omega_0 t\,\mathrm{d}\omega_0 t \\[2mm] &= \frac{4}{\pi}\left[\int_0^{\pi/2} \omega_1 A\sin^2\omega_0 t\,\mathrm{d}\omega_0 t - \int_0^{\pi/2} \frac{\omega_1^3 A^3}{6}\sin^4\omega_0 t\,\mathrm{d}\omega_0 t \right] \\[2mm] &= \frac{4}{\pi}\left[\omega_1 A \cdot \frac{\pi}{4} - \frac{\omega_1^3 A^3}{6} \cdot \frac{3}{8} \cdot \frac{\pi}{2} \right] \end{aligned} \tag{13}$$

$$N(A) = \frac{B_1}{A} = \omega_1 - \frac{\omega_1^3 A^2}{8} \tag{14}$$

In view of the physical meaning of frequency characteristics, the system in Fig. 1 is equivalent to the system shown in Fig. 2.

Effects analysis of nonlinear feedback driven by sine function is discussed as follows.

(1) Effect on the steady state of the closed loop system.

Let the reference input be a step signal, its amplitude is r, the steady state error to the step input is obtained directly by the final value theorem as given below:

$$\begin{aligned} e(\infty) &= \lim_{s\to 0} \frac{s}{1+GKN(A)} \frac{r}{s} \\[2mm] &= \lim_{s\to 0} \frac{r}{1+\left(\dfrac{1}{T_1 s} + \rho \dfrac{K_0}{s(T_0 s+1)} \right)\omega_1} = 0 \end{aligned} \tag{15}$$

Therefore, the nonlinear feedback driven by the sine function has no extra effect to the steady state of the close loop system.

(2) Effect on the dynamic performance of the closed loop system.

The transfer function from the input r (i.e. the setting course ψ_r) to the output y of the system (i.e. the heading angle ψ) is presented as Eq. (16).

$$\frac{y}{r} = \frac{GKN(A)}{1+GKN(A)} \tag{16}$$

For the course keeping control task, wave action is a high frequency disturbance whose frequency spectrum lies in the range of 0.3 ~ 1.25 rad/s. Generally $\omega_1 = .25$ rad/s ($\omega_1 < 0.3$) is taken in Eq. (14) to shy away the wave frequency spectrum. Suppose the range of course changing is between 0 ~ 2π rad,

then $0 < N(A) \leq \omega_1$. Loop Shaping algorithm of H_∞ robust control theory is a kind of open-loop gain shaping method (Zhang, 2012), its key point lies in finding a control law K to make the gains $\underline{\sigma}(GK)$ and $\overline{\sigma}(GK)$ of the open-loop transfer matrix *GK* satisfying the robust performance requirement in the low frequency zone and the robust stability in the high frequency zone, i.e. high gain in the low frequency zone and low gain in the high frequency zone. Loop shaping algorithm implements the closed-loop performance of the system through selecting weighting functions to shape the open-loop frequency characteristic curve, and obtains an acceptable performance/robustness trade-off. According to the loop shaping theory, if Eq. (16) is compared to the closed loop transfer function $GK/(1 + GK)$ of a standard feedback system, the introduction of $N(A)$ does not have much effect to the dynamic performance of the system because of the high gain of *GK* in the low frequency zone and $0 < N(A) \leq 1$.

(3) Effect on the control output of the closed loop system.

The transfer function from the input *r* to the control output δ (i.e. the rudder angle) is shown in Eq. (17), where the nonlinear function $N(A)$ is approximated to ω_1 on condition of the first order item in Eq. (7).

$$\frac{\delta}{r} = \frac{K\omega_1}{1+GK\omega_1} = \frac{\omega_1}{K_0}\frac{s(T_0s+1)}{Ts_1+\omega_1} \qquad (17)$$

To facilitate the following analysis, the control law with the PD form is employed in the further calculation, which can be obtained by directly using the closed loop gain shaping algorithm (2). Substituting the linear model (3) and the original control law (2) into Eq. (17) The corresponding magnitude function is presented in Eq. (18), which is employed to describe its magnifying or compressing power in different frequencies. In Eq. (18), ω is the frequency variable and $\omega \in (0, +\infty)$, while ω_1 is constant parameter for the nonlinear feedback design (see Fig. 1). From the Eq. (18), it is noted that the influence of ω_1 is weak to the gain of $M_{\delta/r}(\omega)$ when ω is with the small value in $(0, +\infty)$. Though, its influence increases as the frequency ω is large or $\omega \to +\infty$. The impact of ω_1 in second part is negligible. Therefore, the gain factor ω_1/K_0 becomes critical in terms of rudder activity saving for $\omega_1 < 1$.

$$M_{\delta/r}(\omega) = \left|\frac{\delta(s)}{r(s)}\right|_{s=j\omega} = \frac{\omega_1}{K_0}\sqrt{\frac{T_0^2\omega^4+\omega^2}{T_1^2\omega^2+\omega_1^2}} \qquad (18)$$

Actually, similar analysis as for Eq. (18) can proceed showing the merits of the nonlinear feedback technique (i.e. the effect of the parameter ω_1) when the control law (5) or (6) is employed. In addition, similar processing technique is common in fuzzy control, neural network and GA optimizing algorithm.

(4) Analysis of simulation results.

Taking the training ship "YULONG" of Dalian maritime university as an example, whose particulars are: Length between perpendiculars $L = 126.0$ m, Beam $B = 20.8$ m, displacement $\nabla = 14\,278.1$ m^3, draught $D = 8.0$ m, block coefficient $C_b = 0.681$, distance from center of mass to the origin of *x* axis $x_c = -3.38$ m, ship speed $U_0 = 15$ kn, rudder area $A_\delta = 18.8$ m^2. The maneuverability indices of the nonlinear Nomoto model $(\ddot{\psi} + \frac{K_0}{T_0}(\alpha\dot{\psi} + \beta\dot{\psi}^3) = \frac{K_0}{T_0}\delta)$ for ships can be calculated from the above parameters (Zhang and Guan, 2010): $K_0 = 0.48$ s^{-1}, $T_0 = 216.58$ s, $\alpha = 9.16$, $\beta = 10\,814.30$. The linear Nomoto model is used to design the robust PID control law, while the nonlinear Nomoto model is employed to carry out the simulation experiment. In the experiment, the parameters in the controller design are as follows: $\rho = 2$, $T_1 = 3$ s, which makes the effective working bandwidth frequency of the course keeping controller being $1/3$ rad/s to avoid overlapping with the wave disturbance range. Rudder servo system is also considered in the simulation, the steering engine is modeled as a system with single hydraulic circuit analog control variable (Zhang, 2012), the maximum rudder rate is $\pm5°/s$ and the saturation rudder angle is $\pm35°$.

When the ship is navigating on the sea, the sway motion and the heading deviation are caused mainly by wind and wave disturbance, therefore the effects of wind and wave cannot be neglected in the simulation. For the wind disturbance, it is divided into the average wind and impulse wind. The impulse wind is implemented using white noise while the average wind is related with the leeway and is expressed as an equivalent rudder angle δ_{wind}. According to the reference (Zhang, 2011; Zhang, 2012), δ_{wind} can be computed by an empirical formula as shown in Eq. (19).

$$\delta_{wind} = K^0 (\frac{V_R}{U_0})^2 \sin\gamma \qquad (19)$$

where K^0 is the coefficient of leeway, V_R the relative wind speed to the ship, U_0 the ship speed, γ the wind angle on the bow. When the wind scale is Beaufort No. 6 and the wind angle on the bow is $-30°$, the equivalent rudder angle of wind can be calculated out as $\delta_{wind} = 3°$.

For the wave disturbance, a simplified model is used which is a second-order oscillating system driven by a white noise, and the transfer function of the wave model under the wind scale of Beaufort No. 6 is given in Eq. (20).

$$h(s) = \frac{0.4198s}{s^2 + 0.3638s + 0.3675} \qquad (20)$$

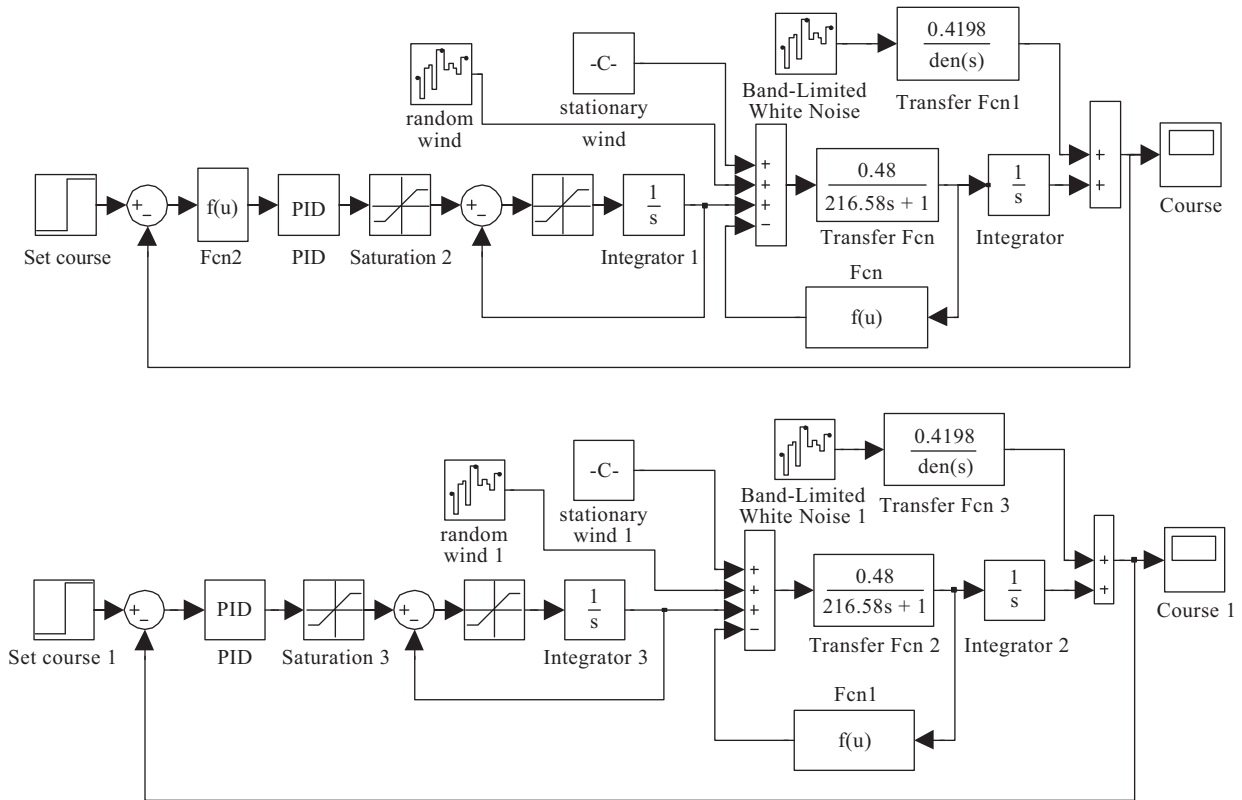The white noise with noise power 0.0001 is simulated by

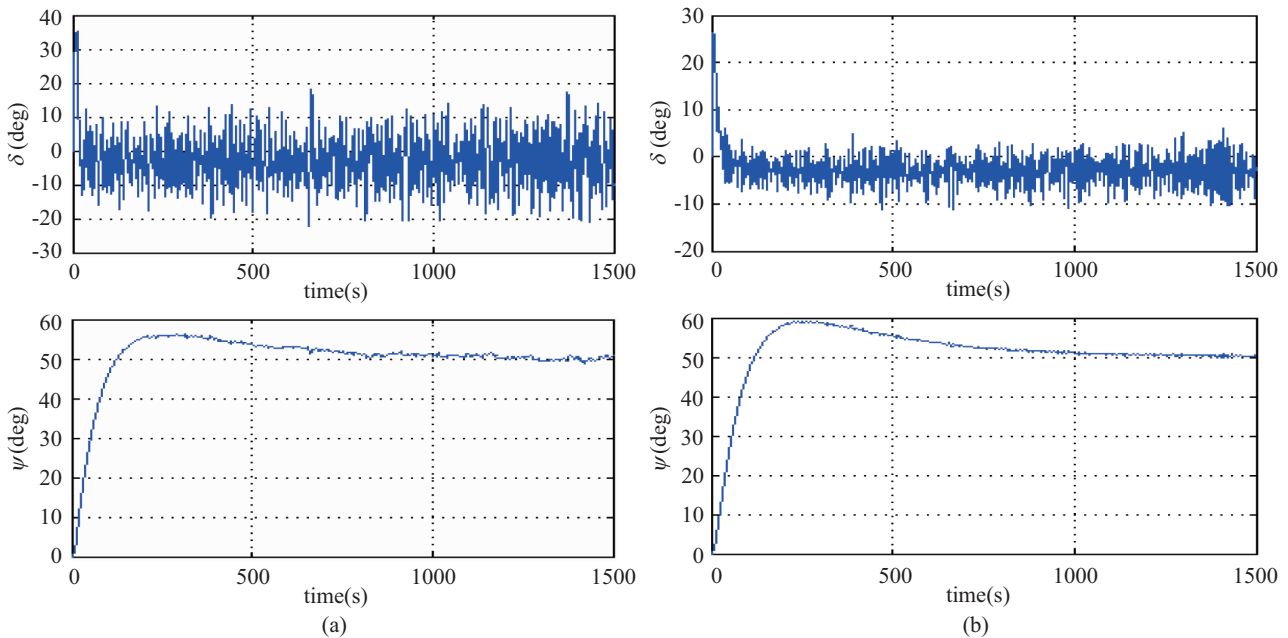Fig. 3. Simulation diagram of Simulink.

Fig. 4. Simulation results of standard feedback (a) and nonlinear feedback (b).

sample time of 0.5 s, which is same to that in the simulation of random wind.

The simulation diagram implemented in Simulink is shown in Fig. 3, the setting course is 50°, and the wind scale is

Beaufort No. 6. Simulation results are shown in Fig. 4. It is noted that the control effect of nonlinear feedback driven by sine function is almost the same as that in standard feedback (the maximum overshoot is increased to 18% from 12%) while
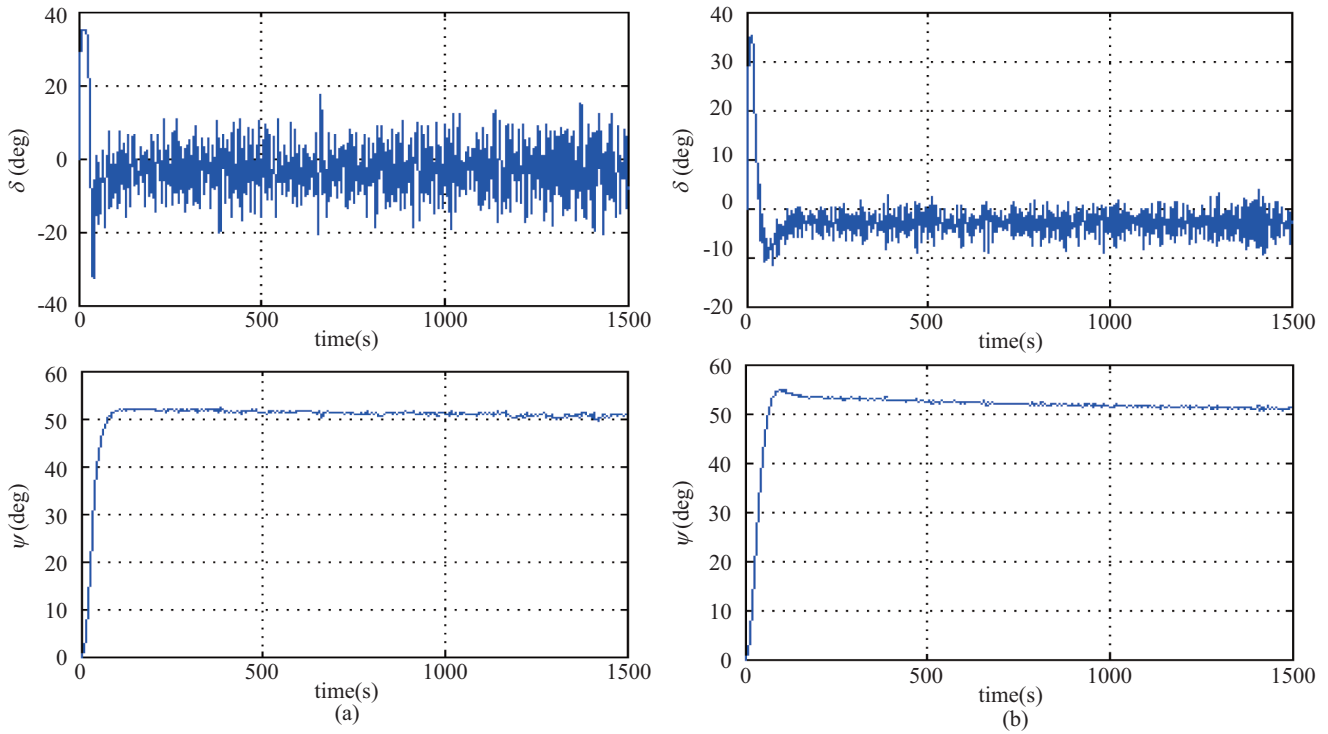
Fig. 5. Simulation results of improved dynamic performance of standard feedback (a) and nonlinear feedback (b).
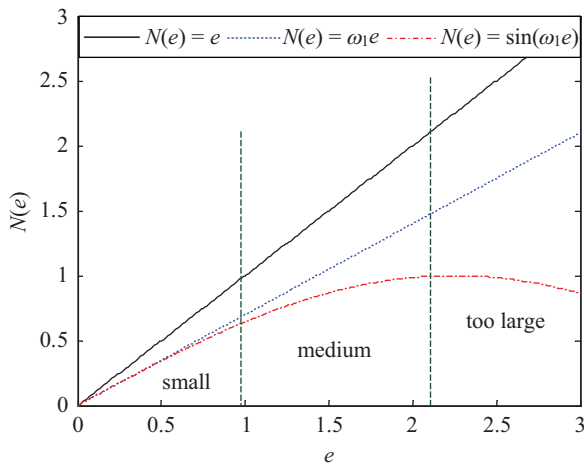

Fig. 6. Comparison of the modulating functions: $N(e) = e$, $N(e) = \omega_1 e$ and $N(e) = \sin(\omega_1 e)$.

the initial maximum rudder angle is reduced to 26.4° from the original 35°. There is 24.6% drop in the initial rudder angle and 45% drop in the average rudder angle which is decreased to an average 3.56° from 6.48°. In a heavy sea state, steering with large rudder angles can cause the amplitude of roll to increase the probability of cargo damage and decrease the comfort index of seafarers as well as the safety coefficient of ship. Therefore, to reduce the amplitude of rudder angle means that the ship will navigate more safely besides its energy saving. In the research mentioned above, a linear

Nomoto model is used for the design of the course keeping controller, and a nonlinear Nomoto model with rudder servo dynamics is applied in the simulation. This is equivalent to adding a kind of perturbation to the model in the simulation study. The satisfactory control effect under the perturbed model demonstrates that the proposed controller is robust to a certain degree.

Parameters used in the design of the controller can be regulated to $T_1 = 4$ s and $\rho = 5$ if the dynamic performance is to be improved further. The corresponding simulation results are shown in Fig. 5. Compare Fig. 5 to Fig. 4, the rise time is reduced to 66 s from the original 122 s; the maximum overshoot of the standard feedback is dropped to 4% from 12% while the maximum overshoot of the nonlinear feedback is decreased to 9.6% from 18%. The average rudder angle of the standard feedback control is also 6.48°, while the average rudder angle of the nonlinear feedback control is 3.65° with 44% drop. The initial rudder in Fig. 5 is enlarged to 35° with better dynamic performance of the controller. If safer navigation is considered which requires smaller initial rudder angle then the control parameters in Fig. 4 are selected. Otherwise, the control parameters in Fig. 5 are used when one wants to obtain better dynamic performance of the system.

In addition, Fig. 6 gives the comparisons of the modulating functions $N(e) = e$, $N(e) = \omega_1 e$ and $N(e) = \sin(\omega_1 e)$. As shown in Fig. 6, it can be concluded that: the control performance of the nonlinear feedback $N(e) = \sin(\omega_1 e)$ is equivalent to that of the linear feedback with an extra constant gain ω_1 when the error $e = r - y$ is small; the performance of the nonlinear

feedback is superior to that of the linear feedback with an extra constant gain ω_1 when the error e is medium; the nonlinear feedback technique cannot work effectively when the error e is too large. It is a very important conclusion that the improvement of control performance is at the cost of the reduction of the system robustness for both schemes.

III. CONCLUSION

In this paper a novel nonlinear feedback control technique is presented. In the scheme, the control error is modulated by a sine function and then is considered as the input of the control law, instead of the original direct error. The nonlinear feedback control could obtain the same stabilizing effect with the minor control action under the original control law. The motivation of this work is not to improve the controller's output performance, but the initial control action. In this note, the average rudder angle is decreased to 3,56° from 6.48°, a 45% drop, while the closed loop performance keep almost same to that in the linear feedback control. The algorithm has the advantages of energy saving and safety in navigation. The same conclusion can be drawn when the nonlinear feedback is used in some other industry plants. Furthermore, the algorithm has some universality. The nonlinear feedback technique could obtain the same control effect by employing the power function $0.1\text{sgn}(r-y)|r-y|^{0.6}$ instead of the $\sin(\omega_1(r-y))$. Though, the nonlinear feedback technique needs to be used prudently when the reference signal is large.

ACKNOWLEDGMENTS

REFERENCES

Bennet, S. (1979). A History of Control Engineering 1800-1930. Peter Peregrinus, London.

Benneff, S. (1984). Nicholas Minorsky and the automatic steering of ships. IEEE Control Systems Magazine 4, 10-15.

Du, J., C. Guo, S. Yu and Y. Zhao (2007). Adaptive autopilot design of time-varying uncertain ships with completely unknown control coefficient. IEEE Journal of Oceanic Engineering 32, 346-352.

Fossen, T. I. (2011). Handbook of Marine Craft Hydrodynamics and Motion Control. Wiley, New York.

Ginoya, D., P. D. Shendge and S. B. Phadke (2015). Disturbance observer based sliding mode control of nonlinear mismatched uncertain systems. Communications in Nonlinear Science and Numerical Simuation 26, 98-107.

Ho, W. H., C. H. Hsieh and J. H. Chou (2010). Optimal course handing control for nonlinear ship maneuvering systems. International Journal of Innovative Computing, Information, and Control 10, 4379-4388.

Hu, S. (2007). Automatic control principle. Science Press, Beijing.

Ihle, I. A. F., J. Jouffroy and I. Fossen Thor (2006). Formation Control of Marine Surface Craft: A Lagrangian Approach. IEEE Journal of Oceanic Engineering 31, 922-934.

Marino, R. and P. Tomei (2013). Global adaptive regulation of uncertain nonlinear systems in output feedback form. IEEE Transactions on Automatic Control 58, 2904-2909.

Satpati B., I. Bandyopadhyay and C. Koley (2008). Robust controller design for course changing / course keeping control of a ship using PSO enabled automated quantitative feedback theory. TENCON 2008-2008 IEEE Region 10 Conference, Hyderabad, 1-6.

Sorensen Asgeir, J. (2011). A survey of dynamic positioning control systems. Annual Reviews in Control 35, 123-136.

Ueno, M., Y. Tsukada and Y. Kitagawa (2014). Rudder effectiveness correction for scale model ship testing. Ocean Engineering 92, 267-284.

Velasco, F. J., E. R. Herrero, E. Lopez, and E. Moyano (2013). Identification for a heading autopilot of an autonomous In-Scale Fast Ferry. IEEE Journal of Oceanic Engineering 32, 263-274.

Zhang, X. and X. Wang (2010). Concise nonlinear robust control of course keeping for ships. ICIC Express Letters 4, 1263-1268.

Zhang, X. (2011). Control algorithm of autopilot driven by sine function of course deviation. Navigation of China 34, 1-5.

Zhang, X. (2012). Concise robust control for ships. Science Press, Beijing.

Zhang, G, X. Zhang and W. Guan (2014). Stability analysis and design of integrating unstable delay processes using the mirror-mapping technique. Journal of Process Control 24, 1038-1045.

Zhang, X., and W. Guan (2010). Improved concise robust control of course keeping for ships with large inertia. Navigation of China 33, 1-5.